Tomographic Three-dimensional Reconstruction of Insect Flight Muscle Partially Relaxed by AMPPNP and Ethylene Glycol

Holger Schmitz,* Mary C. Reedy,‡ Michael K. Reedy,‡ Richard T. Tregear,§ and Kenneth A. Taylor*

*Institute of Molecular Biophysics, Florida State University, Tallahassee, Florida 32306-4380; ‡Department of Cell Biology, Duke University Medical Center, Durham, North Carolina 27710; and §MRC Laboratory of Molecular Biology, Hills Road, Cambridge CB2 2QH, United Kingdom

Abstract. Rigor insect flight muscle (IFM) can be relaxed without ATP by increasing ethylene glycol concentration in the presence of adenosine 5′-[β′γ-imido]triphosphate (AMPPNP). Fibers poised at a critical glycol concentration retain rigor stiffness but support no sustained tension ("glycol-stiff state"). This suggests that many crossbridges are weakly attached to actin, possibly at the beginning of the power stroke. Unaveraged three-dimensional tomograms of "glycol-stiff" sarcomeres show crossbridges large enough to contain only a single myosin head, originating from dense collars every 14.5 nm. Crossbridges with an average 90° axial angle contact actin midway between troponin subunits, which identifies the actin azimuth in each 38.7-nm period, in the same region as the actin target zone of the 45° angled rigor lead bridges. These 90° "target zone" bridges originate from the thick filament and approach actin at azimuthal angles similar to rigor lead bridges. Another class of glycol-PNP crossbridge binds outside the rigor actin target zone. These "nontarget zone" bridges display irregular forms and vary widely in axial and azimuthal attachment angles. Fitting the acto-myosin subfragment 1 atomic structure into the tomogram reveals that 90° target zone bridges share with rigor a similar contact interface with actin, while nontarget crossbridges have variable contact interfaces. This suggests that target zone bridges interact specifically with actin, while nontarget zone bridges may not. Target zone bridges constitute only ~25% of the myosin heads, implying that both specific and nonspecific attachments contribute to the high stiffness. The 90° target zone bridges may represent a preforce attachment that produces force by rotation of the motor domain over actin, possibly independent of the regulatory domain movements.

Force production by myosin heads during muscle contraction has long been modeled as a transition of attached crossbridges from a 90° to a 45° axial angle. Efforts to image crossbridge forms and angles intermediate between 90° heads in ATP-relaxed insect flight muscle (IFM)[1] and the 45° angled bridges in rigor have used nucleotide analogs such as adenosine 5′-[β′γ-imido] triphosphate (AMPPNP) in stable equilibrium states to drive the crossbridges backwards from the 45° angle in rigor to an attached 90° preforce form, otherwise similar to myosin heads in ATP-relaxed fibers (Reedy et al., 1988; Tregear et al., 1990). However, AMPPNP alone will not fully relax IFM, and crossbridges binding AMPPNP retain many rigor-like features (Schmitz et al., 1996; Winkler et al., 1996). On the other hand, AMPPNP in combination with ethylene glycol will relax IFM. When poised at a critical glycol concentration, muscle stiffness is as high as rigor, suggesting crossbridge attachment, but fibers will not bear sustained tension (Clarke et al., 1984; Tregear et al., 1984). Two-dimensional (2-D) analysis of electron micrographs showed that this stiff glycol-PNP state resembled ATP-relaxed fibers in having dense collars every 14.5 nm along the thick filament and thin crossbridges originating from these collars at various axial angles around 90°. However, unlike relaxed muscle, stiff glycol-PNP fibers showed both 90° angled bridges that were regularly spaced every 38.7 nm and more intensity on the 19.3-nm layer line in optical and x-ray diffraction patterns (Reedy et al., 1988; Tregear et al., 1990).

Address all correspondence to Kenneth A. Taylor, Institute of Molecular Biophysics, Florida State University, Tallahassee, FL 32306-4380. Tel.: (850) 644-3357. Fax: (850) 561-1406. E-mail: taylor@bio.fsu.edu

1. *Abbreviations used in this paper*: 2-D and 3-D, two- and three-dimensional; AMPPNP, adenosine 5′-[β′γ-imido]triphosphate; aqueous-PNP, aqueous solution of AMPPNP (without ethylene glycol); glycol-PNP, mixtures of ethylene glycol and AMPPNP; IFM, insect flight muscle; S1, myosin subfragment 1.

Crossbridges in this partially relaxed, glycol-PNP state are important because they may represent the form of the initial attachment of myosin with bound nucleotide preceding force generation (Marston and Tregear, 1984; Tregear et al., 1984; Reedy et al., 1988). This putative preforce 90° crossbridge could not be characterized in 3-D because its variable form and lattice arrangement precluded imaging by averaging methods of 3-D reconstruction. Recently, nonaveraging tomographic methods have been developed and successfully applied to rigor and aqueous-PNP, facilitating characterization of variable crossbridge forms that occur in situ (Taylor and Winkler, 1995, 1996; Schmitz et al., 1996; Winkler and Taylor, 1996).

IFM is superb for structural study because the symmetry and spatial arrangement of filaments results in paired crossbridges on opposite sides of the actin filament. This in turn has given rise to a unique shorthand terminology. The individual crossbridge forms are not unique to IFM, only their symmetrical placement about the thin filament. The filament arrangement also facilitates the microtomy of a type of thin section with coplanar filaments that provide views of the entire crossbridge. The best of these, the myac layer, is a 25-nm-thick longitudinal section containing alternating myosin and actin filaments. In rigor, the maximum number of myosin heads attach to actin, forming doublet pairs every 38.7 nm, the "double chevrons" (Reedy, 1968). "Lead bridges," which form the pair proximal to the M-band, consist of both heads of a myosin molecule and show an overall axial angle of 45° (Taylor et al., 1984). "Rear bridges," which form the pair proximal to the Z-disk, consist of a single myosin head angled closer to 90°. Crossbridges originate from the thick filament along helical tracks so the azimuths of their origins follow a regular pattern. Relative to the thin filament in the myac layer, the lead bridges originate from the left-front and back-right of the adjacent thick filaments, while rear bridges originate from the left-back and right-front. At their actin ends, the crossbridge attachments follow the changing rotation of the actin protomers along the actin helix. The combination of the azimuth of the origin and the azimuth of the crossbridge contact to actin define the azimuthal angle of the crossbridge.

Target zone is the name given to the region of the thin filament where crossbridges bind (Reedy, 1968); by implication this is the region of the thin filament where actin monomers are most favorably placed for actomyosin interaction. In our previous 3-D reconstructions of rigor and aqueous-PNP (Schmitz et al., 1996; Winkler et al., 1996), it was recognized that troponin maintained a constant position with respect to the most regularly positioned crossbridges, the lead bridges, and could thus be used as a landmark to determine the actin dyad orientation in the lead bridge target zone. The most sterically favorable actin position for crossbridge binding in the IFM lattice is midway between troponin densities, where lead bridges bind. The strained structure of the rigor rear bridges suggests that they bind at the very edge of the target zone (Schmitz et al., 1996; Winkler et al., 1996). The target zone defined by lead bridges alone is narrower than target zones previously considered for rigor muscle (Reedy, 1968) because it does not include rear bridge targets.

When aqueous AMPPNP was added to rigor IFM, the tension dropped by two thirds, but the stiffness remained as high as rigor. This initially suggested a reversal of the power stroke, but 3-D reconstructions revealed that the lead bridges remained attached, midway between troponin densities, at axial and azimuthal angles close to rigor. The drop in tension without a large change in axial angle seemed to contradict the lever arm hypothesis for motion producing force. However, a cause for the loss of tension was found in tomograms, which showed that rear bridges detached and were replaced by nonrigor bridges bound to actins outside of the rigor target zone, to sites not selected by crossbridges even under the high-affinity conditions of rigor. These nontarget bridges in aqueous-PNP had variable axial and azimuthal angles and appeared to bind actin with variable contact interfaces. This suggested that they were nonspecifically bound to actin. Moreover, their variable structure did not suggest how a simple axial angle change could convert them to a familiar form, such as an angled rigor bridge.

However, an intriguing doublet crossbridge group with a consistent structure was recognized in aqueous-PNP. Immediately M-ward of the "lead" rigor-like bridge was a "nonrigor" bridge bound at a 90° or antirigor angle. In this doublet, called a mask motif, both lead and M-ward nonrigor bridge pairs had similar azimuths and contact interfaces with actin and bound within the lead bridge target zone. A simple angle change could convert the M-ward, nonrigor bridge in a mask motif to a single headed lead bridge. Thus, in the mask motif, the lead bridge could be at the end of the power stroke, with the M-ward, nonrigor bridge near the beginning. The pairing of rigor and antirigor angled crossbridges bound to the same target zone suggests that crossbridges might act as a relay during muscle contraction (Schmitz et al., 1996).

The affinity of myosin for actin in aqueous-PNP is high compared with weak binding intermediates thought to represent the beginning of the power stroke (Green and Eisenberg, 1980; Biosca et al., 1990). Therefore, the M-ward crossbridge in the mask motif may not represent the best candidate for a preforce crossbridge. Thus, it is important to characterize crossbridge structure in a state with lower actomyosin affinity, such as the stiff glycol-PNP state, where earlier 2-D analysis indicated that weakly attached 90° bridges are prevalent (Reedy et al., 1988). In this work, we have used two spatially invariant features, troponin position and lead crossbridge origins, to identify distinct classes of crossbridges. The invariant position of troponin recognized in 3-D reconstructions allows us to identify the lead bridge target zone and the actin dyad orientation relative to the bound crossbridges. In addition, the "front-back" rule for the azimuth of the origins of the lead target zone bridges distinguishes crossbridges that bind actin with the correct azimuth for specific binding from those that bind nonspecifically. By fitting the myosin subfragment 1 (S1) atomic structure to the in situ bridges, we can compare the positions of the motor and regulatory domains. Previous results and models have introduced the idea that during a power stroke, the crossbridge rotates over the actin binding site while acting as a long, relatively rigid lever arm (Huxley and Simmons, 1971), while others propose that the motor domain position remains constant and light chain domain movements provide a shorter lever

arm (Rayment et al., 1993*b*; Whittaker et al., 1995). Our previous results (Reedy et al., 1987, 1988; Schmitz et al., 1996; Winkler et al., 1996) and the present work show (*a*) that regulatory domain position can vary significantly while motor domain position remains constant and (*b*) that the motor domain can bind actin with varying orientations. This work supports the possibility that both rotation of the motor domain on actin and movements of the regulatory domain could contribute to the power stroke.

Materials and Methods

Specimen Preparation and Electron Microscopy

The embedded fibers used to collect sections and images for these 3-D reconstructions were the same fibers of glycerinated dorsal longitudinal flight muscle of *Lethocerus* prepared in the experiments of Reedy et al. (1988) at 5°C (cold glycol-stiff state). These were bundles of two or three fibers mounted on a tension transducer to measure stiffness and tension during the exposure of the fibers to glycol-PNP. Primary fixation was carried out while the fibers were mounted on the transducer, and then they were removed and processed for EM. Parallel experiments under similar conditions were monitored by x-ray diffraction (Tregear et al., 1990). Tilt series micrographs were obtained at magnification of 18,500 on a Phillips EM 420 (Mahwah, NJ) operated at 100 kV. Images were digitized on a microdensitometer (model PDS 1010M; Perkin-Elmer Corp., Norwalk, CT) at a step size corresponding to 1.25 nm with respect to the original object.

Tomography

We reconstructed two myac layers using a protocol for 3-D tomography derived from the same methods used in 2-D crystal image processing (Amos et al., 1982). The reconstruction steps were the same as described earlier (Schmitz et al., 1996). The reconstruction protocol produces a 3-D reconstruction with a resolution of ~4 nm. Each data set comprised a single uniaxis tilt series of 37 images covering the tilt range from 69° to −76°.

Attachment Parameters for Crossbridges

The most important parameters that we can derive to define a particular crossbridge attachment are its angle relative to the filament axis (axial tilt) and its angle of attachment relative to the actin monomer in a plane perpendicular to the filament axis (azimuthal angle). Our reconstructions do not resolve actin monomers, but the information on the azimuth can be inferred from the 3-D maps using the troponin marker to establish the orientation at one axial coordinate and the periodicity of the actin filament to define the expected rotation as the axial coordinate changed. Troponin could be identified clearly in averaged images of glycol-PNP, thereby defining one point in orientation space independent of crossbridges. Previous work with rigor IFM showed that troponin epitopes were positioned close to the rigor rear crossbridge (Reedy et al., 1994).

3-D reconstructions of rigor IFM revealed that the part of troponin that formed a bump or bead was positioned on a rigor myosin binding site (Taylor et al., 1989*a,b*). Moreover, averaged 3-D reconstructions of both rigor and AMPPNP-treated muscle show that troponin position does not change between these two states (Winkler et al., 1996). Thus, troponin can be used as a marker, independent of the crossbridges to define the actin dyad orientation and the azimuth of the rigor myosin binding site on actin within the reconstruction. With this position thus defined, it is then possible to determine the long pitch helical azimuth at any place on a thin filament. The azimuthal angle of attachment in glycol-PNP was determined mostly for the motor domain part of attached crossbridges since thick filament origins are obscured by additional mass from crossbridges that are not attached to actin and lie close to the thick filament.

Fitting of Atomic Coordinates and Surface Representation

Modeling of the acto-S1 atomic structure into the envelope of the 3-D reconstructions was done starting with the Cα coordinates for a five-subunit actin filament with one S1 molecule attached (kindly provided by Dr. I. Rayment, University of Wisconsin, Madison, WI). From these coordinates, we built a 14 monomer actin filament saturated with S1 molecules and placed it within the reconstruction envelope using the O x-ray crystallography program (Jones et al., 1991). For model construction, the helical operator for a 28/13 helix was used. The atomic coordinates are those for a rigor actomyosin complex, with a uniform angle between S1 and actin and a rigor conformation of the S1 head. However, rigor is significantly different from glycol-PNP, necessitating a fitting procedure in the present work that is somewhat different from that used previously (Schmitz et al., 1996). The first step in the fitting procedure was to select a contour threshold for the reconstruction that would just envelope the atomic coordinates of the actin filament in crossbridge free regions of the thin filament between the troponin complexes. The second step was to obtain an initial alignment of the model structure with the reconstruction. Because of the large structural differences between rigor and glycol-PNP, initially we matched the alignment of the actin dyad orientation and an S1 in the atomic model with the actin dyad orientation and troponin bump in the reconstruction. This defined the actin dyad orientation and azimuth of S1 binding even though the atomic model and glycol-PNP structures were different. After defining the actin dyad orientation based on troponin, we aligned other S1s with the envelopes of the crossbridges.

Our model atomic coordinates were those of fully decorated acto-S1. However, thin filaments in situ are not fully decorated because there are insufficient myosin heads to label all the actins. The excess S1 heads in the model structure that did not superimpose or lie close to the in situ crossbridges were removed from the display, and those remaining heads that were close to the in situ crossbridges were positioned with minimal axial and azimuthal changes from the orientation indicated by the initial alignment.

Because crossbridges in the glycol-stiff state depart significantly from the rigor form, we gave ourselves more flexibility in the fitting process than used in previous work (Schmitz et al., 1996; Winkler et al., 1996). The rigor structure of the S1 molecule was never changed. However, we did change the rigor relationship between actin and S1 using a somewhat constrained movement of the S1 molecule. We allowed the azimuth of contact between S1 and actin and the attachment angle to vary while preventing, as much as possible, a rotation of the S1 about an axis through the motor domain (torsional movement). We minimized torsional movement in the fittings, but in some cases a small amount occurred. At this stage in our analysis, we do not feel that our data are of sufficient resolution to either support or rule out torsional movement of S1 on actin so that the small amount seen in the figures should be considered incidental to the analysis and not significant.

Essentially the same procedure was used for nontarget zone crossbridges, except that the S1 molecule had to be shifted azimuthally from the rigor binding site to overlap the crossbridge envelope. We minimized torsional movement of S1 for the nontarget zone crossbridges for the reasons given above.

Surface representations of the reconstructed maps were obtained using the Explorer software package (Silicon Graphics, Mountain View, CA). All data processing calculations were done on Silicon Graphics Indigo2 computers with Extreme and Solid Impact graphics.

Results

2-D Projections of the Tomogram

The 2-D projection of the glycol-PNP 3-D reconstruction resembles ATP-relaxed muscle in many ways (Fig. 1 *C*). Foremost are the collars around the thick filament spaced at intervals of 14.5 nm that include regularly arranged myosin heads that are not attached to actin and thin crossbridges projecting toward the thin filament with various axial angles whose distribution is centered around 90°. Fig. 1 *A* shows, at higher magnification, that the crossbridges emerge from the collars to attach to the thin filament. The filtered image of the projection (Fig. 1 *C*, *inset*, *bottom right*) emphasizes the annular collars every 14.5 nm around the thick filament.

Unlike relaxed muscle, crossbridges connect to the thin filament at intervals of 38.7 nm. Often, these 90° crossbridges are arranged in rows at the same transverse level

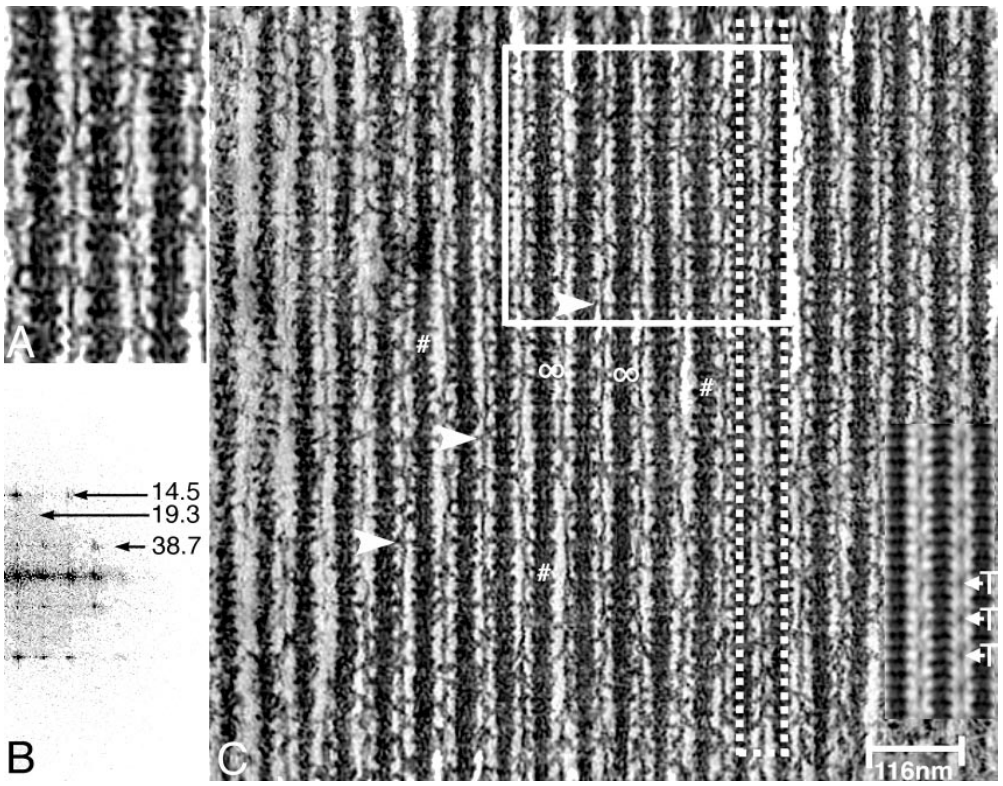

Figure 1. (*A* and *C*) 2-D-projection of a 3-D tomogram of IFM fixed in glycol-PNP. Both the image and its transform (*B*) appear quite similar to those of original EMs taken at 0° specimen tilt. The full size of the actual reconstruction is about 0.8 × 0.8 μm. The pattern of attached crossbridges shows many variations but nevertheless expresses two periodicities. The 14.5-nm repeat marked by dense collars along thick filaments is the most regular feature. The enlargement in *A* makes clear that most crossbridges originate from these collars. The more regular crossbridge attachments favor thin filament sites laterally aligned in transverse rows and axially spaced every 38.7 nm, as marked by arrowheads. These more regular bridges favor angles near 90°. Regions of an actin filament where crossbridges attach on only one side are marked by #. The white-framed area in *C* is the region chosen for the surface representation in Fig. 2. The dotted frame indicates where azimuths of crossbridge origin and attachment were determined for Fig. 5. The small insert at the lower right is a 2-D average of the reconstruction. *T*, troponin complex. Z-line is at the bottom.

(Fig. 1 *C*, *white triangles*). Note also regions where the actin filament is contacted by crossbridges only along one side (Fig. 1 *C*, # on adjacent thick filament), a feature that is seldom seen in relaxed muscle. In the average, the crossbridges are deemphasized, indicating a relatively large disorder in their structure. Particularly prominent in the average are dots spaced every 38.7 nm along the actin filament. These dots are the troponin complex (Fig. 1 *C*, *T*). Thus, troponin as well as the collars on the thick filament are much more regular features than the crossbridges.

"Mask motif" doublets, first observed in AMPPNP-treated IFM (Schmitz et al., 1996), are rare in the glycol-stiff state, but a few can be seen in the 2-D projection (Fig. 1 *C*, ∞). Rather more frequent are partial mask motifs consisting of rigor and nonrigor crossbridges positioned on only one side of the thin filament.

The computed diffraction pattern (Fig. 1 *B*) shows an important feature of the transform of the glycol-stiff state: spots on the 19.3-nm layer line. In relaxed muscle, the 19.3-nm layer line is absent or very weak. In those states of IFM that have significant crossbridge attachment, the 19.3-nm layer line is relatively strong in comparison to relaxed muscle, so that this feature is associated with periodic crossbridge attachment.

Surface Relief of the Glycol-PNP Tomogram

To display details of the reconstruction, we have selected and enlarged a typical region from the very large area imaged in the tomogram. This selected area is indicated by a white square in Fig. 1 and is shown in surface view in Fig. 2 *A*. On the left hand side of Fig. 2 *A* (*dark gray*), three thick filaments (*1*, *3*, and *5*) and the two intervening thin filaments (*2* and *4*) have been averaged only along the filament axis and aligned with the unaveraged tomogram (*light gray*). The average facilitates identification of the 14.5- and 38.7-nm repeats, which can be observed by sighting across the figure from the left hand edge. Thick and thin filaments 1 and 2 on the left are simple averages, while averaged thick and thin filaments 3, 4, and 5 are superimposed with the unaveraged tomogram of the same filaments.

Although the overall crossbridge arrangement in the glycol-PNP state is less ordered than rigor, some regularities, such as the troponin position, are detected and emphasized in the averages (Fig. 2 *A,* filaments *1* and *2*). The position of the troponin complex on the thin filament (Fig. 2 *A*, *T*) can be identified by a lump that coincides with the dark dot seen in the averaged projection. The importance of the troponin position is that it allows us to identify the actin dyad azimuth in the lead bridge target zones. Lead bridge target zones of rigor and AMPPNP-treated muscle are located midway between two successive troponin densities (Schmitz et al., 1996; Winkler et al., 1996). In between the troponin densities are regularly placed bridging bars (Fig. 2 *A, dashed white line*) that represent the "target zone" crossbridges.

The unaveraged tomogram shows bridging densities reaching from the thick to the thin filaments that tend to align in transverse rows spaced axially at 38.7-nm intervals

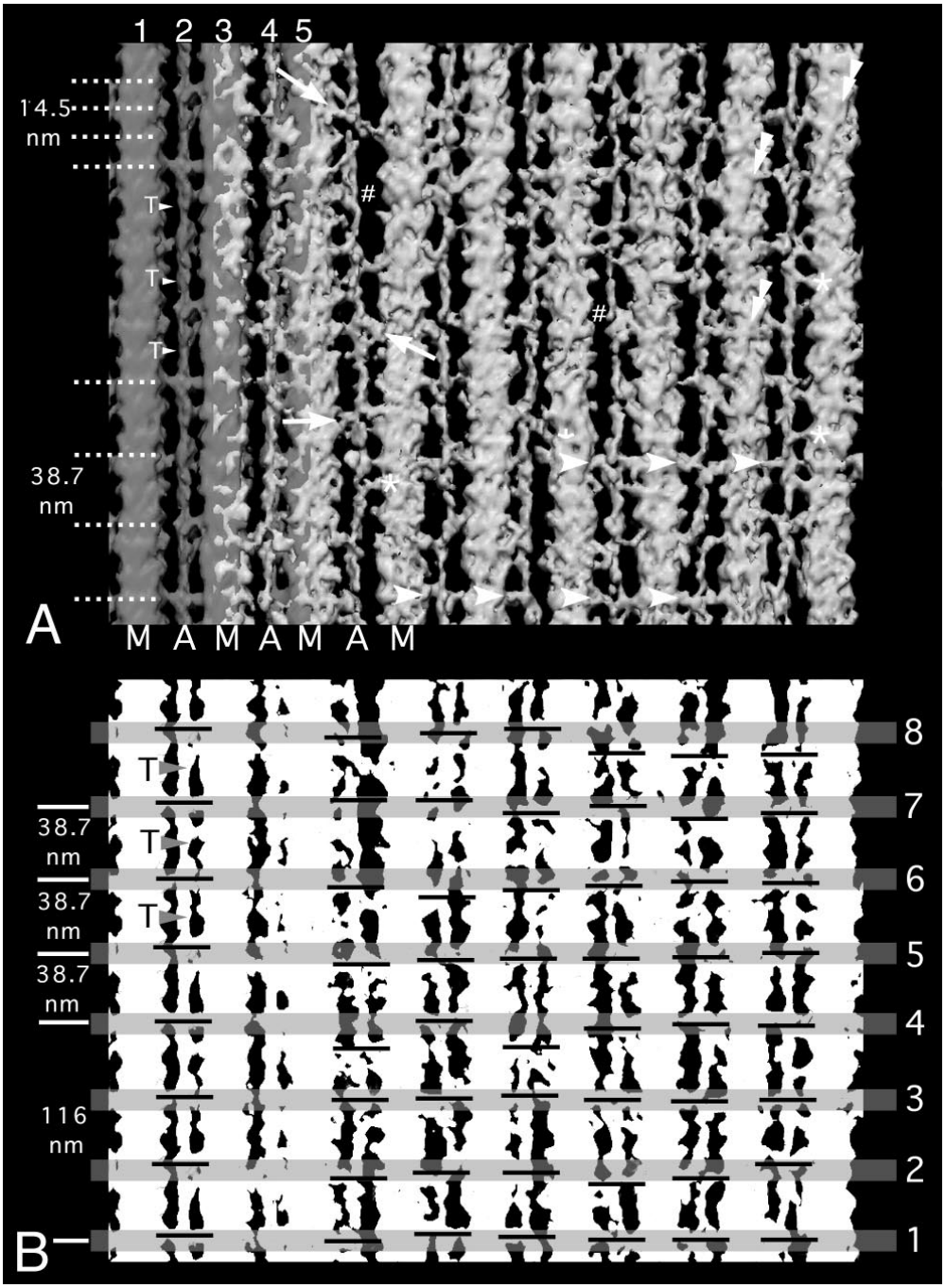

Figure 2. (*A*) Surface rendering of the white-framed area in Fig. 1. *Light gray*, unaveraged tomogram; *dark gray*, averaged filaments replacing or superimposed on the same filaments of the original tomogram averaged only along the y-axis. In the superimposed region, wherever the unaveraged tomogram displays mass that does not appear in the average, the extra mass is shown in light gray. *M*, myosin filament; *A*, actin filament; *T*, troponin complex. A 14.5-nm repeat of crossbridge collars is visible on the thick filament even without averaging. The troponin landmark, best detected in the averages, is identified every 38.7 nm along thin filaments. Target zones in glycol-PNP fall midway between troponin sites. These are the same levels (*A*, *dotted lines* at lower left; *single arrowheads* at lower center and right) occupied by the regular crossbridge attachments noted in Fig 1. The narrow zone of regular attachment indicates that target zones in glycol-PNP are more axially restricted than rigor, apparently because rear bridge targets are not favored. Target zone bridges vary in angle around 90° (reflected by the angle of *white arrows*). Nontarget zone bridges (*) attach between target zone levels and their structure is highly variable. Extended stretches that lack bridges are fairly common (#). Actin filaments are often off center where asymmetry of crossbridge attachments is pronounced. Z-line is at the bottom. (*B*) Target zone crossbridge attachments mapped onto white silhouette of *A*. Horizontal black bars mark levels where semiregular near-90° crossbridges attach to target zones, whose locations were determined by the position of troponin in the average. Horizontal gray stripes mark levels of target zones, positioned midway between troponin bumps, in axial average on left. Black lines represent the actual attachments at or near those actin target zones. Most of the time, these lines fall into the gray regions, showing that the rows of 38.7-nm crossbridges attach in the rigor lead bridge target zone. However, a few attachments fall outside the target zones (rows *4* and *8*). Registration of axial average with underlying and adjacent filaments is computed, not manual. The gray stripes fit well to levels of individual target zones across the adjacent tomogram, but for best reading of troponin repeat and actin azimuth on single filaments (as in Fig. 5), the local average of that filament is used.

(Fig. 2 *A*, *arrowheads*) and that coincide with the dashed white lines in the average. These "target zone" crossbridges generally attach actin at angles of ~90°, although we are able to detect large deviations from this value (Fig. 2 *A*, *arrows* indicating attachment angle; see also Fig. 5). In addition, many crossbridges attach to actin in between those 38.7-nm intervals, and these bridges attach at various angles and azimuthal positions (Fig 2 *A*, *asterisks*). These intermediate crossbridges we refer to as "nontarget zone" bridges. The relative distributions of target and nontarget bridges are best seen when the target zone is marked on an outline image (Fig. 2 *B*). Target zone cross-

bridges are sufficiently well ordered that they are retained in the averages, whereas nontarget zone crossbridges are generally averaged out. Note that where the average and unaveraged filaments in the reconstruction are superimposed, much of the mass (*light gray*) that is averaged out is associated with these less regularly arranged crossbridges.

Most glycol-PNP bridges are smaller than rigor crossbridges, an observation that would suggest that they consist predominately of a single myosin head. Fairly long stretches occur where crossbridges attach on only one side of the thin filament (Fig. 2 *A*, #). On the myosin filament surface, the 14.5-nm period of crossbridge collars is obvious and in some locations, long pitch helical tracks on the thick filament are visible (*double arrowheads*). The averaged myosin filament surface emphasizes the 14.5-nm collars around the thick filament backbone (Fig. 2 *A*, *upper left*, *dashed line*).

Selected Crossbridge Motifs

To illustrate the major aspects of the reconstruction, we selected a gallery of crossbridge structures (Fig. 3). In each panel, the position of the lead bridge target zone is marked with an asterisk on the thin filament. In nearly all cases, the sizes of the crossbridges suggest that they hold only one myosin head.

Target zone crossbridges are most frequently attached at an axial angle of 90° (Fig. 3, *A*, *B*, and *D*); however, the angle can vary from a rigor-like 45° angle (Fig. 3 *E*) to an antirigor 120° angle (Fig. 3 *C*). In some cases, two heads, apparently from different myosin molecules, are seen attaching to adjacent actin monomers (Fig. 3 *D*). In cases such as this, the target zone crossbridge can be identified using the front-back rule (see below). In nearly all cases, the attachment of opposite crossbridges are staggered, reflecting the 2.75-nm stagger of actin monomers on opposite long pitch helical strands of the thin filament. Mask-motif doublets (Fig. 3, *H* and *N*) are occasionally seen in the glycol-PNP state, as are partial mask motifs which have crossbridges on only one side of the thin filament (Fig. 3 *G*).

Target zone crossbridges are often distinguished from nearby nontarget zone bridges by their axial position relative to troponin (Fig. 3, *F* and *L*). An additional distinguishing characteristic is the front-back rule illustrated in Fig. 3 *M*. When viewed toward the Z-disk (as shown here), target zone crossbridges approach the thin filament from the front left and the back right. These are the same directions of approach used by lead bridges of rigor and AMPPNP; these strongly bound bridges are considered to be stereospecifically bound to actin. The front-back rule reflects the approximately twofold axial symmetry of the actin filament and the well-defined azimuth associated with stereospecific binding. Glycol-PNP target zone bridges also bind at the same axial position (the lead bridge target zone) and obey the front-back rule. We therefore consider them to bind actin stereospecifically, even though they are weakly bound. Such weakly, stereospecifically bound heads are good candidates for conversion to a strongly bound form via a power stroke. We would suppose that with a change in orientation accompanying a change in biochemical state, these crossbridges could become strong-binding, force-bearing crossbridges.

In contrast, the nontarget zone bridges may be nonspecifically bound. Due to the helical structure of the thin filament, the azimuthal position of each actin monomer changes by 23° every 55Å of axial translation, so crossbridges from successive 14.5-nm collars that originate from similar azimuth on the thick filament would have to undergo large deformations to align the actin binding site to the myosin binding site on their partner actins, which would be rotated to different azimuths in the thin filament. The single crossbridge positioned Z-wards of the target zone in Fig. 3 *M* illustrates this topological problem. Like the target zone crossbridge, it also approaches actin from the front left side. However, this axial position is near that of the stereospecifically bound rear bridge of rigor, which would approach actin from the back left side, not the front. This nontarget crossbridge therefore interacts with a different surface of the actin monomer than do stereospecifically bound rigor rear bridges. Weakly bound nontarget crossbridges may be nonspecifically attached and would be expected to detach and rebind actin in a more favorable location to allow conversion to a strong-binding form.

Each bridge pair in the mask motif of glycol-PNP obeys the front-back rule (Fig. 3 *N*). The target zone bridges on the Z-ward side in the mask motif approach actin from the same directions (front left, back right) as the lead bridges of rigor and AMPPNP. In contrast to nontarget bridges, the M-ward bridges in the mask motif also approach actin from the same directions as the adjacent, Z-ward target zone bridges, even though they originate from different 14.5-nm collars on the thick filament.

Fitting of Acto-S1 Coordinates into 3-D Reconstructions

The crystal structure of actin (Kabsch et al., 1990), myosin S1 (Rayment et al., 1993*a*), and the derived model of acto-S1 (Rayment et al., 1993*b*) allows us to compare the atomic structures with the in situ crossbridges of our tomographic reconstructions. For the fittings, we selected typical crossbridges from the 3-D map and displayed them in three different representations: a 2-D projection of the crossbridge motif, its surface rendering and a wireframe representation overlaid with the acto-S1 coordinates. Fig. 4, *A–E*, shows a target zone crossbridge pair fitted with the acto-S1 model. In surface view (Fig. 4 *A*), the two crossbridges attach with an axial angle of ~80°. Note that these bridges have a cylindrical shape along the full length, unlike the triangular shape of rigor bridges, whose origin at the thick filament is narrow compared with the broader actin end. The fittings confirm that the cylindrical profiles of glycol-PNP crossbridges are large enough to contain only one S1 head.

Many glycol-PNP bridges originate from the dense collars of density every 14.5 nm around the thick filaments. These collars give the thick filaments a wider appearance compared with rigor, and the exact position of the regulatory domain can be difficult to determine. However, the angle of approach of the motor domain and some portion of the regulatory domain can be determined from the 3-D envelope and compared with the atomic S1 structure.

To visualize the differences between the positions and angles of stereospecific rigor S1 compared with those of

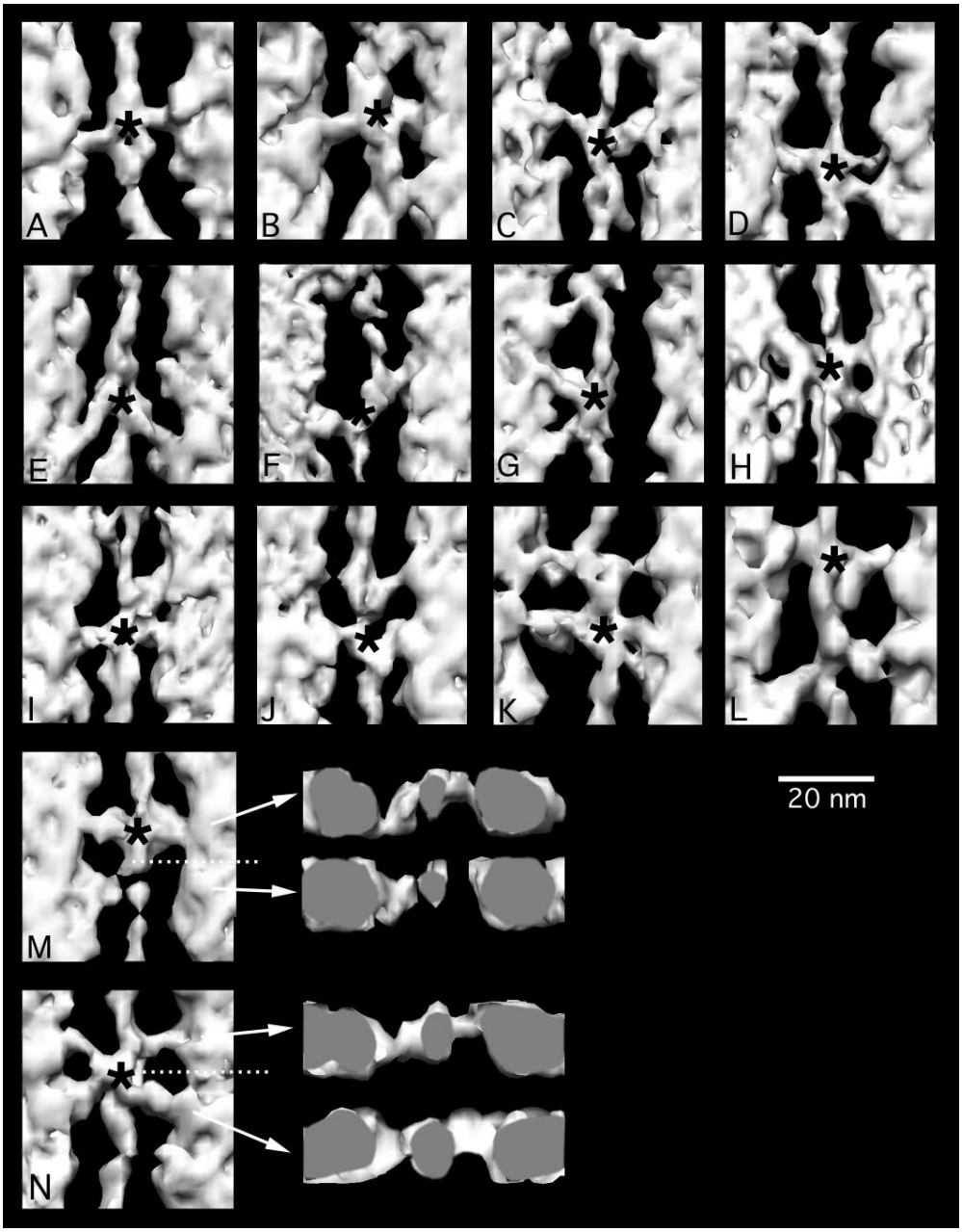

Figure 3. Gallery of glycol-PNP crossbridges. Asterisks mark the axial positions of target zones. *A*, *B*, and *D* typify the most prevalent 90° axial attachment angle of target zone bridges. *C*, *E*, *F*, and *G* show the large axial angle variation that can be detected in target zone bridges. *G* also shows a partial mask motif and an irregular nontarget bridge. (*H*) Complete mask motif. (*I*) 90° target bridge pair and one mask bridge. (*J–L*) show target bridges and variably structured nontarget bridges. (*M*) Target and nontarget crossbridges with transverse view. The azimuth of the origin of the lower nontarget crossbridge in (*M*) and its approach to actin are the same as the upper target zone crossbridge, although the azimuths of their binding sites have rotated 81° and their predicted origins also differ. (*N*) Mask motif in horizontal and transverse view, showing that both bridge pairs originate from the thick filament and approach actin at similar azimuths. Transverse views look toward the Z-line. In longitudinal view, Z-line is at the bottom.

glycol-PNP crossbridges in the reconstruction, a marker of the binding site and angle of rigor S1 have been incorporated into the transverse views (Fig. 4 *B*). This marker (*red*) is kept constant at the rigor binding site and angle even when the S1 molecule has been moved to best match the glycol-PNP crossbridge envelope. Overlaying unmodified rigor acto-S1 on the reconstruction (Fig. 4 *C*) indicates that significant crossbridge mass lies M-ward of the atomic model. Rotating the S1 atomic coordinates from the ~45° rigor angle to near 90° angle (shown in stereo in Fig. 4 *E*) provides a better fit of the atomic structure to the 3-D envelope of the crossbridges in situ. The transverse view (Fig. 4 *D*) shows that the azimuthal position of the glycol-PNP target zone bridges follows that of rigor S1, consistent with a stereospecific attachment of weakly bound, target zone bridges. The transverse views also show that target zone bridge pairs originate from the front left–back right positions, as do rigor lead bridges.

Fig. 4, *F–H*, shows how target and nontarget zone crossbridges differ as seen in longitudinal and transverse view. The pair of target zone crossbridges are attached to the actin filament at an axial angle of ~90° (Fig. 4, *F* and *G*). Above and below are two nontarget crossbridges. Even though in surface view (Fig. 4 *F*) these bridges appear similarly angled, different adjustments of atomic S1 are needed to best match the angle of the crossbridge envelope, seen in Fig. 4 *G*. In the transverse views to the right (Fig. 4 *H*), the target zone crossbridges originate from the left front and back right (obeying the front-back rule) and bind to the same region of actin at similar azimuthal angles as rigor (Fig. 4 *B*). The upper nontarget bridge emerges from the thick filament at the same azimuth as the left target

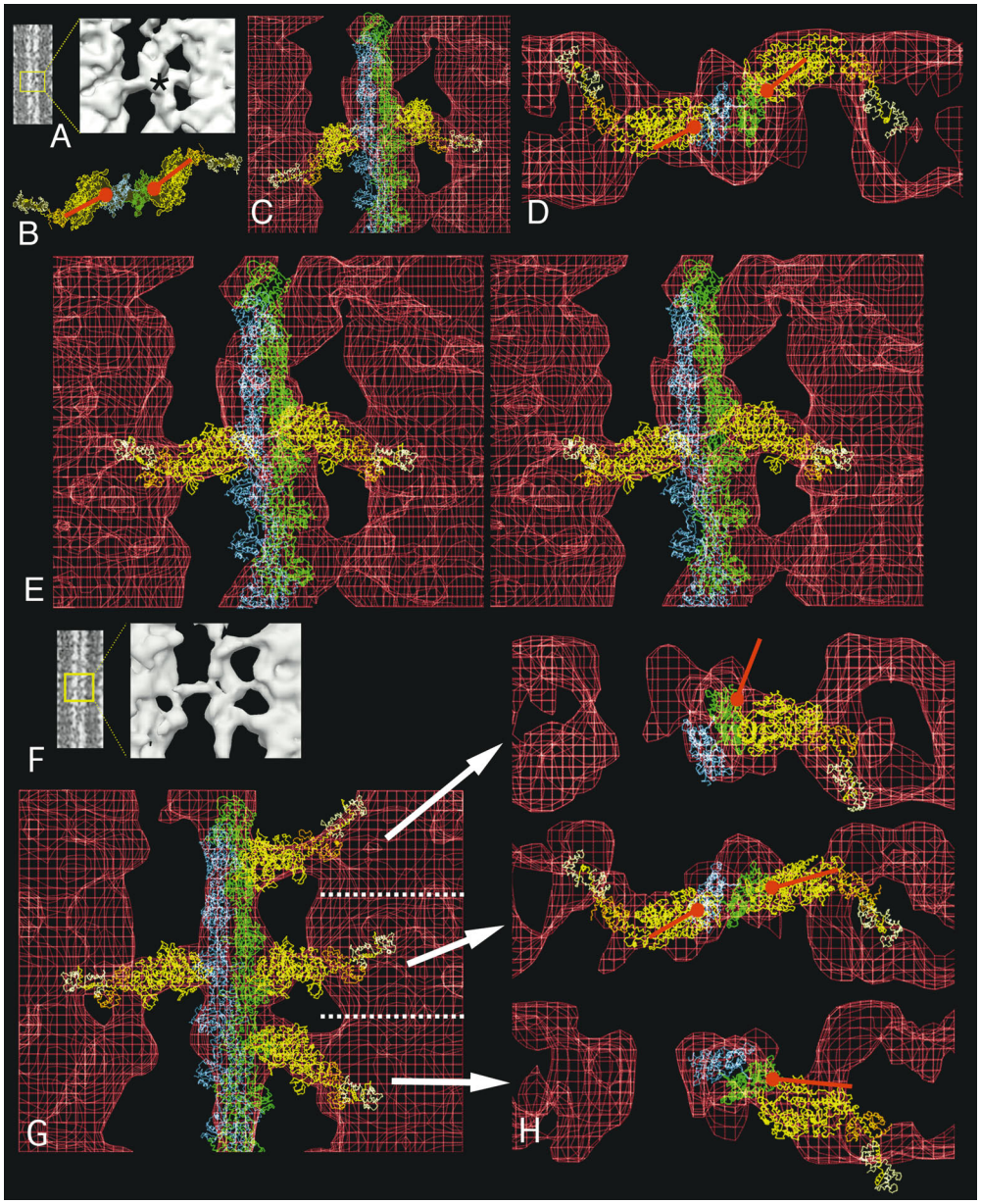

Figure 4. Fittings of the acto-S1 atomic model into target zone and nontarget zone crossbridges of IFM in glycol-PNP. (*A*) Projection image in which the particular motif is boxed and enlarged in the surface view. The asterisk marks the level of the actin target zone. *B* is a view down the filament axis of the rigor atomic model. The orientation of the red ball and stick identify the binding site and azimuthal angle of rigor S1. (*C*) Unmodified rigor acto-S1 model superimposed onto target zone crossbridges shows that the 45° angle of rigor is not matched by the 90° angle of glycol-PNP crossbridges. (*D*) Transverse view of target zone crossbridge seen in *E*, fitted with S1 whose axial angle has been changed to 90°. (*E*) Stereo longitudinal view (ocular divergence) of target zone bridges showing the good fit achieved when the axial angle of S1 is pivoted to 90°. In longitudinal view, the motor domain of the S1 (*C–E*, *yellow*) and the regulatory domain (*orange and white*) fit into the crossbridge envelope (*red*). (*F*) Projection and surface image of a region containing two target zone and two nontarget zone crossbridges. (*G*) Acto-S1 model superimposed on the reconstruction. The orientation of S1 has been changed to align with each crossbridge envelope. (*H*) Transverse view of the same fitting of each of the three crossbridge levels in *G*, showing that while the target zone bridges have similar azimuthal orientation as rigor S1 and bind to the same place on actin, the nontarget bridges do not. In particular, to align S1 with the upper nontarget bridge envelope required moving the actin–S1 interface to a different part of actin.

zone bridge. However, for the nontarget bridge, the axial separation and concomitant helical rotation places the myosin binding site on actin out-of-reach around the thin filament. The apparent contact with actin is at a completely different location from that of rigor crossbridges, whether rear or lead targets. The lower nontarget zone crossbridge is positioned perhaps one actin monomer from the axial position of the rigor rear crossbridge and thus has a somewhat more favorable contact with actin. Previous fittings of rigor rear bridges (Schmitz et al., 1996; Winkler et al., 1996) indicate that considerable distortion of a rigor acto-S1 is needed to position it onto the rear crossbridge. That same kind of distortion is implied here but with a weak-binding glycol-PNP crossbridge. In aqueous-PNP, rigor-like rear bridges are absent. The weak actin affinity of glycol-PNP crossbridges, which tolerate more variation in angle and azimuth (see below) than rigor or aqueous-PNP, may facilitate an actin interaction that is otherwise unfavorable.

Structural Parameters of Glycol-PNP Crossbridges

The azimuth at which crossbridges attach to actin is an important piece of information that is not available from electron micrographs, which are projections, but that can be obtained and quantified from transverse views of a 3-D image. Direct observation suggested that weakly bound glycol-PNP crossbridges showed a wide variety of azi-

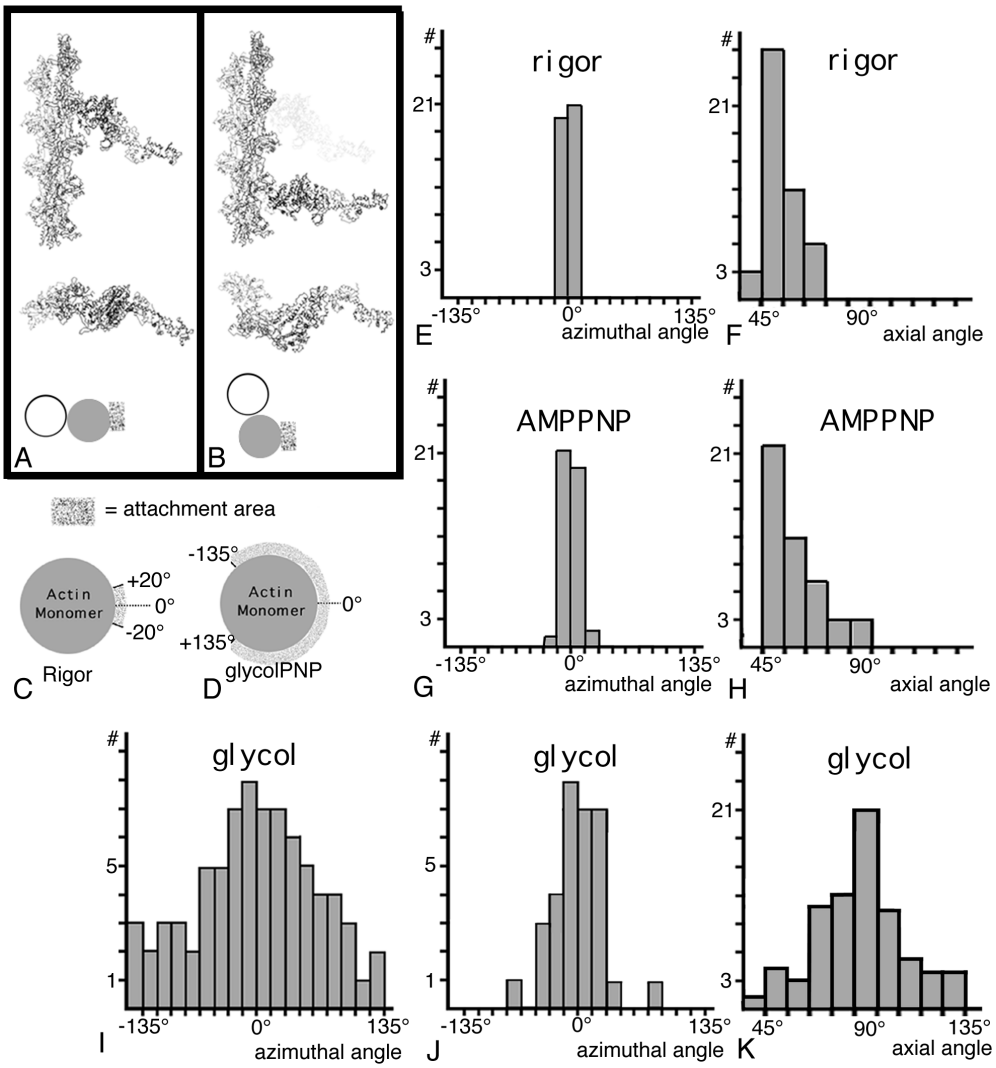

Figure 5. Comparison of the azimuthal and axial orientation of crossbridges in rigor, aqueous-PNP, and glycol-PNP. In *A*, the rigor acto-S1 coordinates are shown in longitudinal and in transverse view in their normal orientation. At the bottom, the shaded rectangle next to the filled circle shows the attachment area, the center of which we give the value of 0.0° as shown in *C*. (*B*) A nontarget zone crossbridge in a position often seen in the glycol-PNP reconstruction, two actin monomers below the lead target zone. The transverse view of *B* shows that the nontarget bridge attaches to a different part of the actin monomer than the rigor bridge in *A*. This azimuthal position would be assigned an angle of 70°. *C* illustrates the narrow range of azimuthal attachment areas on the actin monomer seen in rigor. *D* illustrates the broad range of azimuthal attachment areas when all glycol-PNP crossbridges are included. (*E*) Plot of the narrow distribution of the azimuthal contact of rigor lead bridges to actin. (*F*) Plot of the range of axial attachment angles seen in rigor. (*G*) Aqueous AMPPNP lead bridges also show a narrow azimuthal contact with actin. (*H*) Axial angles of aqueous AMPPNP lead bridges show a spread comparable to rigor but are slightly displaced toward 90°. (*I*) Plot of the distribution of azimuthal angles for all glycol-PNP bridges compared with (*J*) the distribution of target zone bridges only. (*K*) Plot of the range of axial attachment angles for glycol-PNP target zone bridges shows that 90° is the most frequent angle. Data for (*E–H*) were taken from reconstructions previously reported (Schmitz et al., 1996).

muthal attachment angles compared with a narrow distribution in rigor. The problem is illustrated in Fig. 5 *A*, where a rigor S1 is bound to actin according to the Rayment model. In Fig. 5 *B*, a glycol-PNP crossbridge is bound to actin at a different azimuth than rigor. To quantify the azimuthal attachment angles of rigor and glycol-PNP bridges, we selected one actin filament from the present reconstruction that spanned a complete half sarcomere (Fig. 1 *C*, *black and white dotted outline*) and determined the azimuthal position of each attached crossbridge (74 total). The exact orientation of the actin azimuth was determined by the position of the troponin complex in each 38.7-nm repeat, and the observation that this coincides with an S1 binding site (Taylor et al., 1989*a*,*b*). In our analysis, we define the binding azimuth in rigor as 0.0°.

In glycol-PNP, the distribution of azimuthal attachment angles is quite large for all crossbridges and spans a range of ±135° (Fig. 5 *I*). Many of these crossbridges in glycol-PNP are nontarget zone crossbridges whose nonspecific attachment gives rise to the broad angular distribution. The distribution is much narrower for target zone crossbridges (Fig. 5 *J*), with most crossbridge attachments falling within a ±30° arc around the average rigor value. This narrower distribution shows that target zone crossbridges have a more specific actin interaction than the nontarget zone crossbridges. However, the azimuthal angle distribution is much broader than that obtained by the same method for target zone crossbridges in rigor (Fig. 5 *E*) and AMPPNP (Fig. 5 *G)* as determined from our previous reconstructions (Schmitz et al., 1996). Most of the measurements for those states fall within ±20° of the 0.0° value defined for rigor. When rigor rear bridges are added to the rigor distribution (data not shown), the azimuthal distribution shifts very slightly toward a more positive angle.

The axial angle distribution for target zone glycol-PNP crossbridges is very different from that obtained for rigor and aqueous-PNP target zone crossbridges. In rigor, the angles are roughly centered about 45° (Fig. 5 *F*), and for

aqueous-PNP the distribution skewed, with most angles being near 45° but a significant number at angles closer to 90° (Fig. 5 *H*). The axial angular distribution for glycol-PNP crossbridges is centered around 90° (Fig. 5 *K*) but is considerably broad and encompasses both rigor and antirigor angles.

The distribution of azimuthal and axial attachment angles for rigor, aqueous-PNP, and glycol-PNP crossbridges (Fig. 5) reveals an underlying specificity in the actin interaction for target zone crossbridges. For these three states, the azimuthal angle distribution broadens as actin affinity is lowered but still remains centered around the rigor angle. However, the axial attachment angles change, with the center of the distribution approaching 90° as actin affinity is lowered. The data suggest that the actin interaction changes with chemical state of the crossbridges. Moreover, it suggests that the interaction between actin and myosin has specificity to the extent that in all three states, target zone crossbridges are bound to actin at the same interface, but the motor domain has varying angles.

Discussion

The reconstructions reported here are the first 3-D images of in situ crossbridges that are likely to be in a weakly attached state. Near the critical glycol concentration, IFM fibers in glycol-PNP have high mechanical stiffness but will not bear sustained tension, thereby suggesting a weak interaction with actin. Thus, 3-D reconstructions of crossbridges in this mechanical state should provide images of good candidates for preforce crossbridges. The structure of myosin in weakly attached, preforce states has been difficult to identify in the variable images produced by isolated acto-S1 (Applegate and Flicker, 1987; Frado and Craig, 1992; Walker et al., 1995). Even if myosin head form in a weakly bound, preforce state could be preserved and identified in acto-S1, under in vitro conditions the isolated molecules do not produce force, they are not under the constraints enforced by their integration in a lattice of filaments, and stiffness cannot be measured as an assay for attachment. These nonaveraging tomographic reconstructions allow us to observe variable myosin head form in situ and provide a means to analyze them and distinguish the most likely candidates for preforce crossbridge form.

In Glycol-PNP, Target Zone Crossbridges Attach to Actin Stereospecifically, While Nontarget Zone Bridges Attach Nonspecifically

Our previous tomograms of IFM treated with aqueous-PNP (Schmitz et al., 1996) revealed two classes of crossbridges. One class, the lead bridge, was bound to the actin targets of rigor lead bridges. The structure of lead bridges in aqueous-PNP was slightly different from rigor lead bridges. However, lead crossbridges in AMPPNP were bound to the same part of the actin monomer as their rigor counterparts, suggesting that these target zone crossbridges bound specifically to actin. Crossbridges of the second class bound in regions of the thin filament where rigor crossbridges are not observed. Fitting the atomic structure of rigor acto-S1 into the reconstructions revealed that AMPPNP crossbridges in this second class bound to different parts of the actin monomer than rigor bridges suggesting that these nontarget zone crossbridges bound nonspecifically to actin.

In glycol-PNP, both target and nontarget crossbridges are also present. However, target zone crossbridges in glycol-PNP have a structure significantly different from both rigor and AMPPNP target zone bridges. Target zone bridges in glycol-PNP appear exclusively single headed. This is consistent with a model of Geeves and Conibear (1995), in which weak binding of both myosin heads is unlikely because of strain effects. The distribution of tilt angles in glycol-PNP is centered around 90° rather than 45°. However, the change in the tilt angle of glycol-PNP target zone bridges is not accompanied by a change in the azimuth of the thick filament origin; target zone bridges in glycol-PNP originate from similar azimuths on the thick filament as those in rigor and aqueous-PNP. Glycol-PNP target zone bridges also bind to the same region of the actin monomer as rigor bridges. For these reasons, we consider the glycol-PNP target zone bridges to be bound to actin at the interface associated with strong-binding, force-bearing crossbridges. However, the interaction of the target zone crossbridges differs in some details. For example, the azimuthal and axial angular distribution for glycol-PNP target zone crossbridges is broader than for rigor and aqueous-PNP, particularly so for the axial angle. Since the axial angle can take on values both less than 90° (rigor-like) and greater than 90° (anti–rigor-like), it seems unlikely that the motor domain of S1 can be binding actin in a single orientation.

In contrast, nontarget zone crossbridges do not follow an obvious pattern with regard to their thick filament origins. They approach actin from a variety of directions and they bind to actin on different surfaces from that observed in rigor. The nontarget bridges are therefore considered to bind nonstereospecifically to actin.

S1 Fittings Show that Glycol-PNP Bridges Have Different Conformations of the Motor and Regulatory Domains

Fitting S1 into the envelope of target zone bridges reveals that the alignment of the rigor structure required both azimuthal adjustment (rotation about the filament axis) and tilt angle adjustment (rotation about the perpendicular to the filament axis) to superimpose S1 with the reconstruction envelope. The binding site on actin served adequately as the pivot point for these adjustments, although good alignment of the S1 and crossbridge regulatory domains would still require changes in the angle between the regulatory and motor domains, which were not attempted. The motor domains of S1 and target crossbridges were brought into approximate alignment by our adjustments, but the need to pivot S1 about the actin binding site to obtain a reasonable fit implies some alteration in the actomyosin interface compared with that in rigor (and also AMPPNP).

In the case of nontarget zone crossbridges, simply pivoting the S1 about the binding site on actin could not successfully align the S1 atomic model with the reconstruction envelope. Even approximately superimposing S1 on a nontarget bridge required translational movements away from the rigor binding site, indicating that these myosin heads are binding to a different interface on actin.

These fittings of S1 to glycol-PNP crossbridges can compare the relative positions of the motor domains of the bridges to the S1 more easily than the relative positions of the regulatory domains. This is because the light chain domain of a glycol-PNP bridge often merges with the 14.5-nm collars, and its position relative to the S1 regulatory domain cannot be judged. In contrast, the fittings in rigor showed the light chain domain free of the thick filament. However, the fact that glycol-PNP crossbridges extend from the 14.5-nm collars on the thick filament establishes that the regulatory domains must be differently configured than rigor or AMPPNP crossbridges. This also demonstrates that the collars themselves, and not an intermediate point between them, represent the crossbridge origin.

The Maintenance of High Stiffness in Glycol-PNP

Our 3-D reconstructions of rigor, AMPPNP, and glycol-PNP–treated IFM show approximately the same number of attachments from crossbridges to actin despite the rather large structural differences between the states. In rigor, strongly bound target zone attachments dominate, and over 50% of these involve two-headed lead bridges. Virtually all myosin heads in rigor interact with the same region of actin, and this is defined as stereospecific binding. After addition of AMPPNP, actin–myosin affinity is reduced, specifically attached target zone and nonspecific, nontarget zone crossbridges occur, and fewer than 50% of the attachments arise from two-headed crossbridges. In the glycol-PNP state, affinity is further reduced, all crossbridges are one-headed, and only ~50% are target zone bridges. Despite these differences, the isotonic stiffness is the same in all three states (Tregear et al., 1990). This establishes that weakly bound, single-headed crossbridges must contribute significantly to isotonic stiffness. Furthermore, it is possible that, despite the considerable difference in crossbridge structure, the stiffness per crossbridge is approximately the same and independent of whether the crossbridges are classified target zone or nontarget zone. To be otherwise would require that the stiffness per crossbridge increase while its affinity for actin decreased. Our observations are consistent with the theory that stiffness per crossbridge is independent of its state (Schoenberg and Eisenberg, 1987) and would seem to suggest that nonspecifically attached crossbridges make a similar contribution to stiffness as those stereospecifically bound.

Relationship to X-ray Diagrams of IFM

The 3-D reconstruction reveals a distribution of crossbridges in glycol-PNP that can explain the appearance of intensity on the 19.3-nm layer line (10.12 reflection) in x-ray and optical diffraction patterns (Tregear et al., 1990; Reedy et al., 1988). In ATP-relaxed IFM, intensity on the 19.3-nm layer line is not observed (Reedy et al., 1988, 1992). The location of the troponin complex every 38.7 nm along the thin filament gives rise to much of the intensity observed on the 38.7-nm layer line in relaxed IFM. Because the lead bridge target zones are positioned midway between troponin complexes, the additional mass following the actin helix contributed by the regular binding of glycol-PNP crossbridges in target zones will halve the 38.7-nm period, thereby increasing intensity on the 19.3-nm layer line, rather than on the 38.7-nm layer line. On the other hand, the mass of the nonspecifically attached nontarget crossbridges does not follow the actin helix and, therefore, will not contribute significantly to intensity on the 38.7- or 19.3-nm layer lines. X-ray diagrams of contracting IFM show a pronounced increase in the intensity of the 19.3 nm (10.12 reflection) during stretch activation (Tregear, R.T., R.J. Edwards, T.C. Irving, K.C. Poole, M.C. Reedy, H. Schmitz, E. Towns-Andrews, and M.K. Reedy, manuscript submitted for publication). The increase in 19.3 intensity of contracting IFM can also be explained by the regular binding of crossbridges to the lead bridge target zone.

The Transition from Rigor to Stiff Glycol IFM

With these reconstructions of IFM in glycol-PNP, we have 3-D information on a sequence of stable equilibrium states that have a range of crossbridge structure from strongly bound bridges at the end of the power stroke in rigor to weakly attached bridges that may represent the form of myosin heads at the beginning of a working stroke. The three states are shown together for comparison in Fig. 6. Rigor IFM is characterized mechanically by high stiffness and the ability to retain a large imposed tension. In rigor (Fig. 6, *A–C*), there are two crossbridge classes. One class, the lead bridge, contains both heads of a myosin molecule. The myosin heads in the two-headed lead bridge have different structures imposed by their common origin and separate target actins. One head generally appears more angled than the other, giving the crossbridge an overall triangular shape. The single-headed crossbridge class, the rear bridges, have variable angles and are bent azimuthally considerably more than lead bridges. Modeling of the atomic acto-S1 structure into the 3-D images of rigor muscle suggests that rear bridges have a highly strained conformation (Schmitz et al., 1996; Winkler et al., 1996).

On addition of AMPPNP to rigor IFM, tension drops by 70%, but stiffness remains high as in rigor (Reedy et al., 1988). AMPPNP causes detachment of rear bridges and their redistribution to other actin monomers not normally occupied in rigor (Fig. 6, *D–F*). Lead bridges are retained, but their structure is slightly altered from the rigor lead bridges. AMPPNP lead bridges have a rigor tilt angle, except that the regulatory domain region shows a small 0.5–1.0-nm M-ward shift, and the bridges are less azimuthally bent in transverse view (Winkler et al., 1996). Both one- and two-headed lead bridges are present. The glycol-PNP state is characterized by the loss of the remaining tension but little change in stiffness, which remains at or near the rigor level. In the glycol-PNP state (Fig. 6, *G–I*), both the 45° attachment angle and the triangular shape of crossbridges in the lead target zone are lost. Instead, 90° single-headed crossbridges predominate, and the only ordered class of bridges is found bound at the lead bridge target zones.

It is ironic that relative to the 90° to 45° lever arm model, the greatest mechanical change occurs on addition of AMPPNP to rigor IFM, while the angle changes in the target zone crossbridges are minimal. On glycol addition to AMPPNP, the mechanical changes are relatively small, while the structural changes are far more pronounced. The angled, rigor-like lead bridges in AMPPNP are replaced in

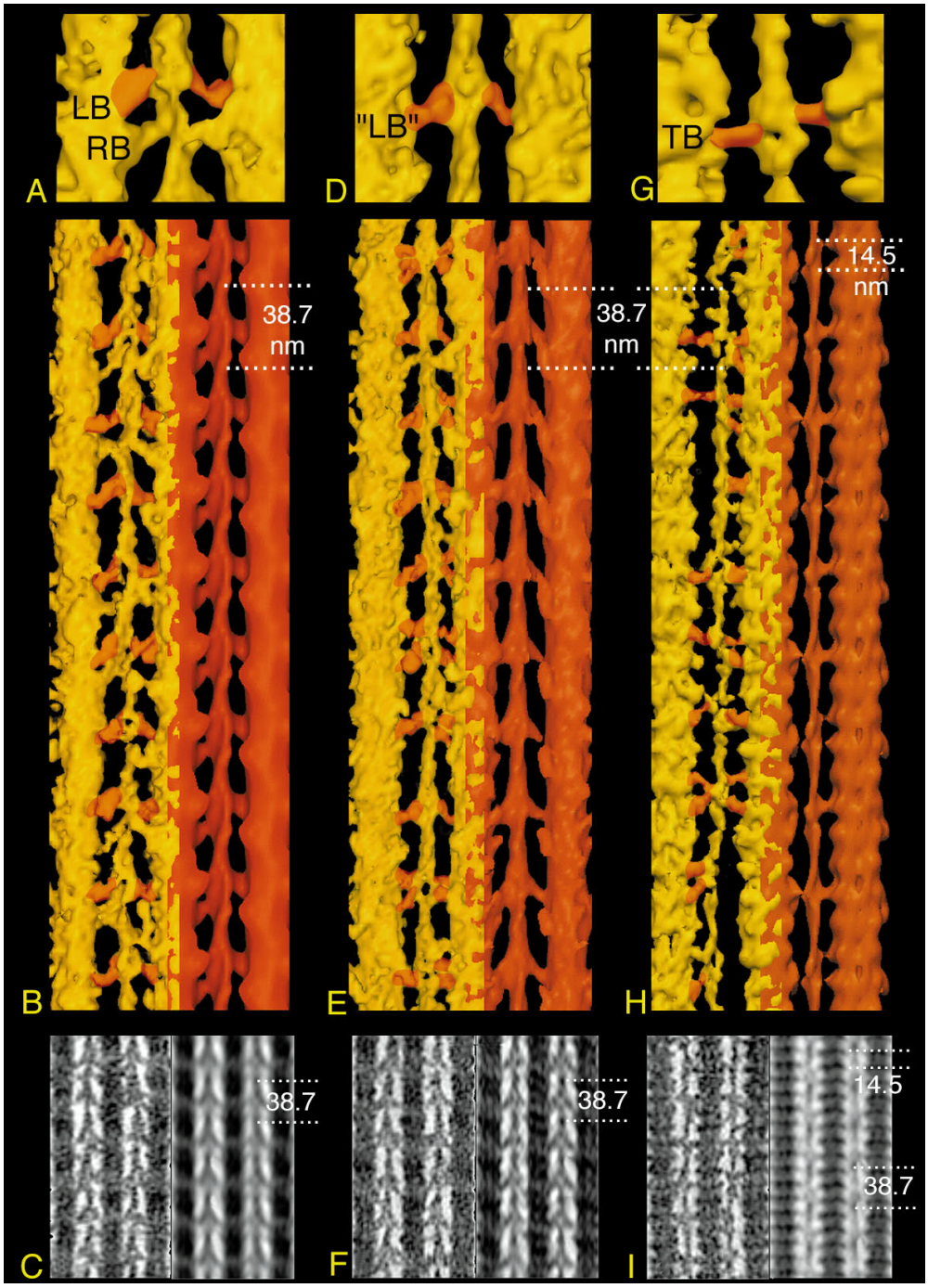

Figure 6. Comparison of 3-D tomographic reconstructions of IFM in three equilibrium states: Rigor (*A–C*) and AMPPNP (*D–F*) (from Schmitz et al., 1996) and the glycol-PNP reconstruction described here (*G–I*). Surface renderings of attached crossbridges at the lead bridge target zone on top, surface rendering of a larger area in the middle and 2-D projections on bottom. The orientation with respect to the muscle is with Z-line on the bottom. In *B*, *E*, and *H*, the axially averaged filament is shown in red to the right of the unaveraged tomogram on the left. In the tomograms, target zone crossbridges are painted orange for ease of identification. The comparison clarifies the main differences among the three states: the rigor state shows well-ordered, double-headed crossbridges arranged in double chevrons consisting of lead and rear bridge pairs every 38.7 nm. The lead bridges, which hold two myosin heads, are attached at a 45° angle, while the smaller, single-headed rear bridges attach on average at a 90° angle. There is no 14.5-nm periodicity visible on the myosin filament surface. In aqueous-PNP, the 45° attached lead bridge motif every 38.7 nm is retained, while rear bridges redistribute to random-like positions. A weak 14.5-nm periodicity can be seen on the myosin filament surface. Lead bridges often appear to be single headed. The glycol-PNP state shows single-headed attached crossbridges every 38.7 nm, but their shape, size, and attachment angle differs from the lead bridges. In addition, many random-like attached bridges can be seen. The myosin filament surface reveals a strong 14.5-nm repeat of crossbridge shelves.

glycol-PNP by a single-headed 90° crossbridge in the lead target zone. The change in angle from 45° to 90° that occurs with minimal sarcomere lengthening indicates that significant crossbridge detachment and redistribution has occurred. These stable states were originally hoped to show a reversal of the power stroke. However, in order for these stages to be viewed as a reverse power stroke, the structural changes must occur in attached crossbridges. As our 3-D reconstructions show, significant crossbridge detachment and redistribution occurs during the transition

from rigor to glycol-PNP. The crossbridge redistribution that is a significant part of the maintenance of stiffness is due to the occurrence of nonspecifically attached, nontarget crossbridges, which must detach and rebind actin in a more favorable location to convert to a strongly bound 45° angle. The importance of such nonspecific, myosin–actin interactions may be the recruitment of crossbridges to the vicinity of the actin filament during active contraction, where they can bind quickly to target zone actin sites when these are brought into favorable alignment by filament sliding.

The sequence from rigor to glycol-PNP shows overall a 45° to a 90° angle change, but the crossbridge forms seen in situ reveal relatively independent changes in axial angle of the motor domain and reconfiguration of the regulatory domain of myosin. The 90° glycol-PNP target zone bridges establish that myosin heads originating from 14.5-nm collars can attach specifically to actin with a nonrigor form and angle. Conversion of the bridges to 45° associated with strong binding could occur by rotation of the motor domain while bound to actin. Such a rotation independent of the regulatory domain could allow the motor domain to develop a strong-binding configuration on actin while building strain in the crossbridge. This possibility provides a mechanism to "cock" the regulatory domain lever arm for the eventual working stroke while at the same time allowing the strong-binding interface to form. The strain could then be released, and a working stroke produced, through independent rotation of the regulatory domain. This aspect distinguishes our interpretation from models that require only a single binding configuration on actin (Rayment et al., 1993) and models that allow rotation of the entire crossbridge on the actin interface (Huxley and Simmons, 1971).

The PDS 1010M densitometer was purchased with funds from National Science Foundation grant PCM-8400167. This work was also supported by DFG grant Schm 1035/1 (H. Schmitz) and National Institutes of Health grants GM-30598 (K.A. Taylor) and AR-14317 (M.K. Reedy).

Received for publication 13 March 1997 and in revised form 10 July 1997.

References

Amos, L.A., R. Henderson, and P.N.T. Unwin. 1982. Three-dimensional structure determination by electron microscopy of two-dimensional crystals. *Prog. Biophys. Mol. Biol.* 39:183–231.

Applegate, D., and P. Flicker. 1987. New states of actomyosin. *J. Biol. Chem.* 262:6856–6863.

Biosca, J.A., E. Eisenberg, M.C. Reedy, and M.K. Reedy. 1990. Binding of ADP and adenosine 5′-[β,γ-imido]triphosphate to insect flight muscle fibrils. *Eur. J. Biochem.* 189:395–399.

Clarke, M.L., C.D. Rodger, and R.T. Tregear. 1984. Modification of crossbridge states by ethylene glycol in insect flight muscle. *J. Muscle Res. Cell Motil.* 5:81–96.

Frado, L.-L., and R. Craig. 1992. Electron microscopy of the actin-myosin head complex in the presence of ATP. *J. Mol. Biol.* 223:391–397.

Geeves, M., and P.B. Conibear. 1995. The role of three-state docking of myosin-S1 with actin in force generation. *Biophys. J.* 68:194S–199S.

Green, L.E., and E. Eisenberg. 1980. Dissociation of the actin-subfragment 1 complex by adenyl-5′-yl imidodiphosphate, ADP, and PPi. *J. Biol. Chem.* 255:543–548.

Huxley, A.F., and R.M. Simmons. 1971. Proposed mechanism of force generation in striated muscle. *Nature (Lond.).* 233:533–538.

Jones, T.A., J.-Y. Zou, S.W. Cowan, and M. Kjeldgaard. 1991. Improved methods for building protein models in electron density maps and the location of errors in these models. *Acta Cryst.* A47:110–119.

Kabsch, W., H.G. Mannherz, D. Suck, E.F. Pai, and K.C. Holmes. 1990. Atomic model of the actin filament. *Nature (Lond.).* 37:44–49.

Marston, S.B., and R.T. Tregear. 1984. Modification of the interactions of myosin with actin and 5′-adenylyl imidodiphosphate by substitution of ethylene glycol for water. *Biochem. J.* 217:169–177.

Rayment, I., W.R. Rypniewski, K. Schmidt-Baese, R. Smith, D.R. Tomchick, M.M. Benning, D.A. Winkelmann, G. Wesenberg, and H.M. Holden. 1993*a*. Three-dimensional structure of myosin subfragment-1: a molecular motor. *Science (Wash. DC).* 261:50–58.

Rayment, I., H.M. Holden, M.C. Whittaker, B. Yohn, M. Lorenz, K.C. Holmes, and R.A. Milligan. 1993*b*. Structure of the actin-myosin complex and its implications for muscle contraction. *Science (Wash. DC).* 261:58–65.

Reedy, M.C., M.K. Reedy, and R.S. Goody. 1987. The structure of insect flight muscle in the presence of AMPPNP. *J. Muscle Res. Cell Motil.* 8:473–503.

Reedy, M.C., M.K. Reedy, and R.T. Tregear. 1988. Two attached non-rigor crossbridge forms in insect flight muscle. *J. Mol. Biol.* 204:357–383.

Reedy, M.C., M.K. Reedy, K. Leonard, and B. Bullard. 1994. Gold/Fab immuno electron microscopy localization of troponin H and troponin T in *Lethocerus* flight muscle. *J. Mol. Biol.* 239:52–67.

Reedy, M.K. 1968. Ultrastructure of insect flight muscle. I. Screw sense and structural grouping in the rigor crossbridge lattice. *J. Mol. Biol.* 31:155–176.

Reedy, M.K., C. Lucaveche, N. Naber, and R. Cooke. 1992. Insect crossbridges, relaxed by spin-labeled nucleotide, show well-ordered 90° state by x-ray diffraction and electron microscopy, but spectra of electron paramagnetic resonance probes report disorder. *J. Mol. Biol.* 227:678–697.

Schmitz, H., M.C. Reedy, M.K. Reedy, R.T. Tregear, H. Winkler, and K.A. Taylor. 1996. Electron tomography of insect flight muscle in rigor and AMP-PNP at 23°C. *J. Mol. Biol.* 264:279–301.

Schoenberg, M., and E. Eisenberg. 1987. ADP binding to myosin crossbridges and its effect on the crossbridge detachment rate constants. *J. Gen. Physiol.* 89:905–920.

Taylor, K.A., and H. Winkler. 1995. 3-D reconstruction of paracrystalline biological specimens by tomography. *In* Proceedings Microscopy and Microanalysis. G.W. Bailey, M.H. Ellisman, R.A. Hennigar, and N.J. Zaluzec, editors. Jones and Begell Publishing, New York. 734–735.

Taylor, K.A., and H. Winkler. 1996. Tomography of paracrystalline specimens. *In* Proceedings Microscopy and Microanalysis. G.W. Bailey, J.M. Corbett, R.V.W. Dimlich, J.R. Michael, and N.J. Zaluzec, editors. San Francisco Press, San Francisco, CA. 586–587.

Taylor, K.A., M.C. Reedy, L. Cordova, and M.K Reedy. 1984. 3-D structure of insect flight muscle in rigor from tilted thin sections. *Nature (Lond.).* 310: 285–291.

Taylor, K.A., M.C. Reedy, L. Córdova, and M.K. Reedy. 1989*a*. Three-dimensional image reconstruction of insect flight muscle. I. The rigor myac layer. *J. Cell Biol.* 109:1085–1102.

Taylor, K.A., M.C. Reedy, L. Córdova, and M.K. Reedy. 1989*b*. Three-dimensional image reconstruction of insect flight muscle. II. The rigor actin layer. *J. Cell Biol.* 109:1103–1123.

Tregear, R.T., C.S. Terry, and A.J. Sayers. 1984. The process of muscle relaxation by the combined action of MgAMPPNP and ethylene glycol. *J. Muscle Res. Cell Motil.* 5:687–696.

Tregear, R.T., K. Wakabayashi, H. Tanaka, H. Iwamoto, M.C. Reedy, M.K. Reedy, H. Sugi, and Y. Amemiya. 1990. X-ray diffraction and electron microscopy from Lethocerus flight muscle partially relaxed by adenylylimidodiphosphate and ethylene glycol. *J. Mol. Biol.* 214:129–141.

Walker, M., J. Trinick, and H. White. 1995. Millisecond time resolution electron cryo-microscopy of the M-ATP transient kinetic state of the acto-myosin ATPase. *Biophys. J.* 68:87S–91S.

Whittaker, M., E. Wilson-Kubalek, J. Smith, L. Faust, R. Milligan, and L. Sweeney. 1995. A 35-Å movement of smooth muscle myosin on ADP release. *Nature (Lond.).* 378:748–751.

Winkler, H., and K.A. Taylor. 1996. Three-dimensional distortion correction applied to tomographic reconstructions of sectioned crystals. *Ultramicroscopy.* 63:125–132.

Winkler, H., M.C. Reedy, M.K. Reedy, R.T. Tregear, and K.A. Taylor. 1996. 3-D structure of nucleotide bearing crossbridges in situ: oblique section reconstruction of insect flight muscle in aqueous AMPPNP. *J. Mol. Biol.* 264:302–322.